

Eco-Friendly Synthesis of Silver Nanoparticles via *Morus Nigra* Extract in Ethanol: A Sustainable Nanomaterial Approach

Renny Nazario-Naveda^{1, a)}, Daniel Delfin-Narciso^{2, b)}, Luisa Juárez-Cortijo^{2, c)},
Moisés Gallozzo-Cárdenas^{3, d)}, and Luis Angelats-Silva^{4, f)}

¹Facultad de Ingeniería y Arquitectura, Universidad Autónoma del Perú, Lima 15842, Perú.

²Grupo de Investigación de Ciencias Aplicadas y Nuevas Tecnologías, Universidad Privada del Norte, Trujillo 13001, Perú.

³Facultad de Ciencias de la Salud, Universidad César Vallejo, Trujillo 13002, Perú.

⁴Laboratorio de Investigación Multidisciplinario, Universidad Privada Antenor Orrego, Trujillo 13008, Perú.

^{a)} Corresponding author: renny.nazario@autonoma.pe

^{b)}daniel.delfin@upn.edu.pe

^{c)}luisa.juarez@upn.edu.pe

^{d)}mmgallozzo@ucvvirtual.edu.pe

^{e)}langelatss@upao.edu.pe

Abstract. In this study, a green synthesis method for silver nanoparticles (AgNPs) was developed using *Morus nigra* (black mulberry) extract in 96% ethanol as a reducing agent and stabilizer. Different extract volumes were evaluated to determine the optimal synthesis conditions. The formation of AgNPs was confirmed by UV-Vis spectroscopy, with characteristic absorption peaks around 420 nm. When using a volume of 3.0 mL, a well-defined peak with greater stability over time was observed, indicating efficient synthesis and a more uniform size distribution. FTIR analysis revealed the presence of phenolic functional groups and anthocyanins in the extract, confirming their role as reducing and stabilizing agents on the surface of the AgNPs. Complementarily, Dynamic Light Scattering (DLS) analysis showed that the nanoparticles obtained with 3.0 mL had a lower average hydrodynamic size and a narrower distribution. In antimicrobial assays, the nanoparticles showed the largest inhibition zones against *Staphylococcus aureus* and *Escherichia coli*.

INTRODUCTION

In recent years, various studies have highlighted the growing interest in silver nanoparticles (AgNPs) due to their distinctive physicochemical properties and their effectiveness against a wide variety of microorganisms. These characteristics position them as promising materials for applications ranging from medicine to food preservation and the treatment of environmental pollutants [1,2]. However, conventional methods used for their synthesis, such as chemical reduction, require toxic reagents and high temperatures, raising environmental concerns and limiting their use in products intended for direct contact with living beings [3]. In this context, the green synthesis of nanoparticles, based on the use of plant extracts as reducing and stabilizing agents, has emerged as a sustainable and environmentally friendly strategy. Green synthesis allows AgNPs to be obtained under mild temperature and pressure conditions, reducing the generation of hazardous waste and energy consumption [4,5]. In addition, the secondary metabolites present in the extracts, such as flavonoids, anthocyanins, and phenolic acids, not only facilitate the reduction of Ag⁺ ions to Ag⁰, but also contribute to the stability and surface functionalization of the nanoparticles, improving their biocompatibility [6,7]. On the other hand, a fundamental aspect in the characterization of AgNPs obtained by green synthesis is the analysis of surface chemical interactions by Fourier transform infrared spectroscopy (FTIR), which allows the identification of functional groups present in the extracts that participate in the reduction and stabilization of the nanoparticles. Recent studies have shown that FTIR spectra of AgNPs synthesized with fruit extracts show bands corresponding to hydroxyl (–OH), carbonyl (C=O), and carboxyl (–COOH) groups, confirming the involvement of polyphenols, flavonoids, and anthocyanins as the main agents responsible for the synthesis and stabilization process [8]. These observations coincide with recent research, which highlights how FTIR analysis is essential for understanding the relationship between the natural functionalization of the AgNP surface, its stability, and biological efficacy [1]. In this vein, fruits with high anthocyanin content, such as blueberries, blackberries, and cherries, have

been recognized as effective sources for the green synthesis of AgNPs, thanks to their richness in phenolic compounds with antioxidant capacity [8,9]. For example, extracts from blueberries (*Vaccinium* spp.), particularly *V. oxycoccos*, rich in phenolic compounds such as anthocyanins, have been shown to be effective in the green synthesis of silver nanoparticles (AgNPs). Spherical AgNPs with average sizes in the range of 5–30 nm and an absorption band in the UV-Vis spectrum centered around 450 nm, attributed to well-defined surface plasmons, have been reported. Similarly, extracts from cherries (*Prunus avium*) and raspberries (*Rubus idaeus*) have been shown to produce nanoparticles with controlled sizes, good colloidal stability, and significant antimicrobial effects, highlighting the role of anthocyanins as reducing and stabilizing agents [10,11].

AgNPs produced by green methods exert their antimicrobial activity through mechanisms such as the release of Ag^+ ions, capable of altering bacterial proteins and nucleic acids; the generation of reactive oxygen species (ROS) that cause oxidative damage; and the direct disruption of the cell membrane, leading to the loss of integrity and death of microbial cells [12,13]. For example, biosynthesized nanoparticles showed significant antimicrobial activity against *Escherichia coli* and *Staphylococcus aureus*, attributed to both their small size and the presence of bioactive compounds in the extract that act as natural stabilizing agents. Residual biomolecules, such as anthocyanins, contribute to colloidal stability and enhance interaction with bacterial membranes through steric and electrostatic mechanisms [10]. Complementarily, AgNPs between 10 and 50 nm have been shown to exhibit potent bactericidal action through mechanisms that include the generation of reactive oxygen species, damage to cell membranes, and disruption of essential metabolic processes [13]. However, the effectiveness of these nanoparticles can vary considerably depending on the microbial species and synthesis parameters, such as the type of extract used, the concentration of nanoparticles, and the resulting size, factors that must be optimized to achieve lower minimum inhibitory concentrations and broaden their applicability [3,14].

Morus nigra (black mulberry) is a fruit species characterized by its high content of anthocyanins, flavonoids, and phenolic acids, compounds that act as reducing agents and antioxidants [13]. Research reports that these metabolites not only provide the characteristic coloration of blackberries but also facilitate the reduction of Ag^+ ions and stabilize nanoparticles by preventing their agglomeration, thus providing greater colloidal stability [6,15]. However, the potential of *Morus nigra* extracts for AgNP synthesis has been scarcely explored, opening up an opportunity to develop functional nanomaterials through a sustainable approach. In this regard, this study aims to develop a green synthesis method for silver nanoparticles using *Morus nigra* extract in 96% ethanol, characterize their optical and chemical properties by UV-Vis and FTIR analysis, and evaluate their antimicrobial activity against *Escherichia coli* ATCC 25922, *Staphylococcus aureus* ATCC 29213, and *Candida albicans* ATCC 10231. The aim is to contribute to the development of sustainable nanomaterials with potential applications in the biomedical and environmental fields.

METHODOLOGY

The ripe fruits of *Morus nigra* were harvested fresh, washed with distilled water, and dried at room temperature. Sixty grams of pulp were weighed, crushed, and mixed with 150 mL of 96% ethanol (Laboratorios Dropaksa S.R.L.). The mixture was subjected to ultrasound under standard equipment conditions of 40 kHz and 50 W for 30 minutes. The extract was then filtered through Whatman No. 1 paper and stored at 4 °C in amber bottles until use. This ethanolic extract served as a reducing agent and stabilizer in the synthesis of silver nanoparticles. For the synthesis of Ag NPs, the green chemistry method was used, employing silver nitrate AgNO_3 (Merck -CAS: 7761-88-8) at a concentration of 1mM as the precursor agent. Twenty milliliters of this solution were taken and heated in a thermomagnetic stirrer at 60 °C and 400 rpm for 10 minutes. Next, 2.5 mL of black mulberry extract was added dropwise, and the pH of the mixture was adjusted to 10 by controlled addition of sodium hydroxide (NaOH, Merck, CAS: 1310-73-2), without interrupting the stirring. The resulting solution was allowed to cool in a brown bottle protected from light. This procedure was repeated for other volumes of extract (from 2.5 mL to 4.0 mL). The synthesized AgNPs were stored appropriately for subsequent characterization and testing. The optical properties of the extract and colloidal samples of silver nanoparticles were characterized by UV-Vis spectrophotometry (Shimadzu, UV 1900, Tokyo, Japan) at room temperature, analyzing the presence of the Surface Plasmon Resonance (SPR) peak typical of silver nanostructures. The functional groups were determined by FTIR spectrophotometry (Thermo Fisher Nicolet IS-50). The spectrum of each sample was obtained with 20 scans in a frequency range of 4000 to 400 cm^{-1} with a resolution of 4 cm^{-1} . In addition, dynamic light scattering analysis (Nicomp Nano Z3000) was performed to characterize the size distribution of Ag nanoparticles (NPs). The antimicrobial activity of the nanoparticles was evaluated by microdilution in plates to determine the minimum inhibitory concentration (MIC) against *E. coli* ATCC 25922, *S. aureus* ATCC 29213, and *C. albicans* ATCC 10231. The strains were cultured for 18–24 h at $36 \pm 1^\circ\text{C}$ and adjusted to a turbidity equivalent to the

McFarland 0.5 standard ($\approx 1 \times 10^8$ CFU/mL). Serial dilutions of the nanoparticles were prepared from 100% to 0.4%, and each well was inoculated with 10 μ L of microbial suspension to obtain a final concentration of 1×10^5 CFU/mL. The plates were incubated at $36 \pm 1^\circ\text{C}$ for 24–48 h, and the presence or absence of growth was evaluated. The MIC was defined as the lowest concentration that completely inhibited growth in all replicates.

RESULTS AND ANALYSIS

The UV-Vis spectrum of black mulberry extract in 96% ethanol (Figure 1a) shows broad absorption with defined maxima around 420 to 430 nm and a second absorption region between 500 and 540 nm, suggesting the combined presence of anthocyanins and other phenolic compounds. Anthocyanins, the main pigments responsible for the intense purple color, usually show absorption maxima in the range of 510 to 540 nm in alcoholic solutions, associated with their flavylum structure and the pH of the medium. The peak around 420 nm could correspond to flavonoids and condensed tannins, whose presence has been reported to contribute to the reducing potential of the extract [16,17]. This combination of signals supports the phytochemical richness of the extract, which is key to its use as a reducing and stabilizing agent in green synthesis of metal nanoparticles, given that the conjugation of double bonds and hydroxyl groups favors the transfer of electrons to metal ions [2]. The FTIR spectra obtained for the black mulberry extract (Figure 1b) shows characteristic bands at approximately 3300 cm^{-1} , $2920\text{--}2850\text{ cm}^{-1}$, 1600 cm^{-1} and 1045 cm^{-1} . The broad band around 3300 cm^{-1} corresponds to O–H stretching vibrations, typical of phenolic compounds and flavonoids, which are abundant in black mulberry extracts and reported to have reducing capacity in nanoparticle synthesis [5]. The bands at 2920 and 2850 cm^{-1} are attributed to the C–H stretching of aliphatic chains, suggesting the presence of carbohydrates or fatty acids, while the region near $1600\text{--}1500\text{ cm}^{-1}$ is associated with C=O and C=C vibrations of aromatic and carbonyl compounds [18].

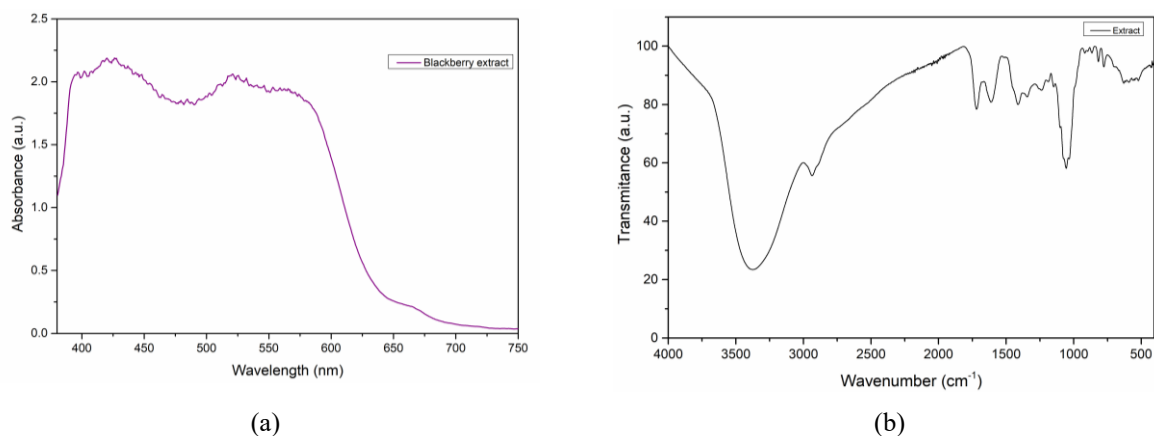


FIGURE 1. (a) UV–Vis absorption. (b) FTIR spectrum of the 96% ethanolic extract of *Morus nigra*.

Characterization by UV-Vis spectroscopy confirmed the formation of silver nanoparticles (AgNPs) using black mulberry extract as a reducing agent at different volumes (2.0 to 4.0 mL). The absorbance values at day 1 are shown in Figure 2a. The presence of the characteristic surface plasmon resonance (SPR) peak in the range of 414 to 420 nm is also reported by various authors for the formation of spherical AgNPs dispersed in colloidal media [19,20]. Results show a slight decrease in the intensity of the characteristic peak for volumes corresponding to 2.5 mL and 3.0 mL compared to 2.0 mL. This decrease is attributed to an inadequate ratio between the reducing agents and the available silver ions, which limits the efficiency of nucleation and growth of metal nanoparticles. Similar results have been reported in studies where the extract/precursor ratio directly influences the nucleation kinetics [21]. On the other hand, for volumes of 3.5 to 4 mL, an increase in the absorbance peak is observed, indicating a greater number of nanoparticles formed. This behavior indicates that at higher extract concentrations, synthesis yield tends to improve and nanoparticle density increases, thanks to the greater availability of reducing and stabilizing agents present in the extracts [22,23]. On the other hand, the SPR peak shift shows a progressive increase towards longer wavelengths (from 414 nm to 420 nm), particularly at higher volumes. This phenomenon can be interpreted as an indication of a slight increase in nanoparticle size or a change in their morphology, since larger or less spherical particles tend to exhibit peaks at longer wavelengths. Therefore, although 4.0 mL shows the highest absorbance, the slight spectral shift suggests that the particle size may not be the most desirable for applications requiring small and well-controlled

sizes [24]. The stability of the AgNPs was verified using UV-Vis spectroscopy six months after synthesis (Figure 2b). All spectra show an additional shift towards red, with SPR peaks between 419.6 nm and 427.4 nm, suggesting an increase in the average size of the nanoparticles during storage. This behavior is characteristic of the Ostwald ripening process, a mechanism in which smaller particles dissolve and their ions redeposit on larger ones, favoring their growth and decreasing their surface energy [25]. Such a phenomenon can occur even in stabilized colloidal solutions, as demonstrated by studies on AgNPs synthesized with plant extracts [5]. It is important to note that, despite colloidal growth, the absorbance intensity remains high and even homogeneous between volumes of 2.5 and 4.0 mL, indicating good optical stability of the AgNPs during storage. This stability has been attributed to the prolonged action of the phenolic compounds present in the extract, which prevent excessive agglomeration [26]. Similarly, Liu et al. have pointed out that the preservation of the optical signal is closely related to the sustained antimicrobial performance of AgNPs, which is relevant for biomedical or agricultural applications [27]. Considering both the initial absorbance intensity and spectral stability after six months, the optimal volume of black mulberry extract for synthesis could be 3.0 mL, as it offers a balance between high nanoparticle production (evidenced by high absorbance), an SPR peak around 425 nm (indicating adequate sizes), and greater spectral homogeneity over the long term.

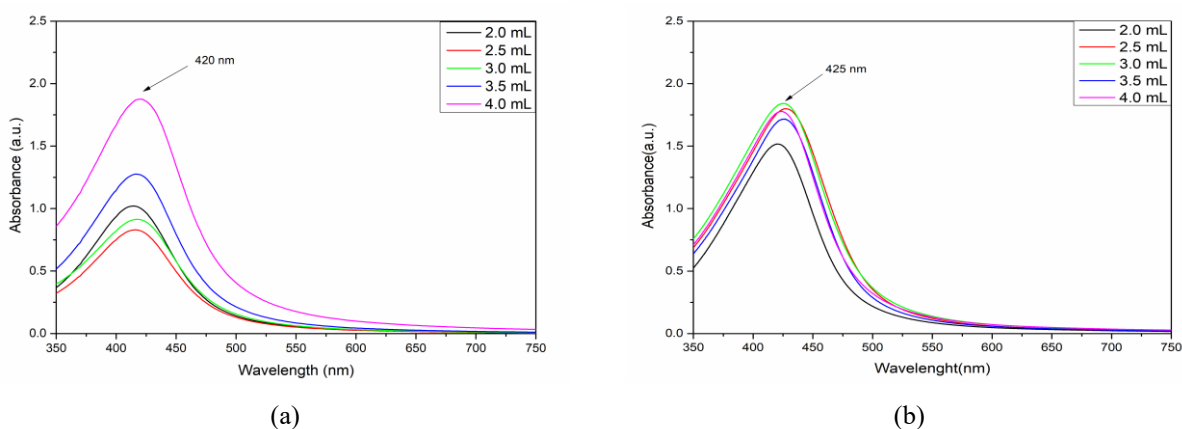


FIGURE 2. UV-Vis absorption spectra of AgNPs synthesized using black mulberry extract as a reducing agent, at different extract volumes at (a) day 1. (b) day 180.

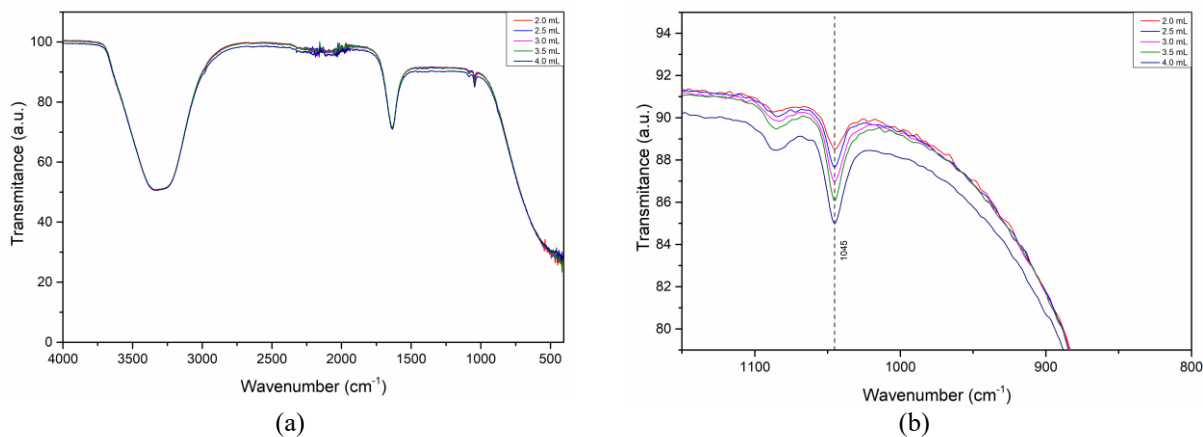


FIGURE 3. (a) FTIR spectra of silver nanoparticles synthesized with different volumes of *Morus nigra* extract (2.0–4.0 mL). (b) FTIR spectrum enlargement showing a peak at 1045 cm⁻¹.

FTIR spectra of AgNPs synthesized with different volumes of the extract (2.0 to 4.0 mL) are shown in Figure 3a. These spectra retain many of the bands observed in the original extract, including the bands around 3300 cm⁻¹, 2920 cm⁻¹ and 1045 cm⁻¹, although with slight variations in intensity and shape. The O–H band remains prominent, suggesting that phenolic groups are still present on the surface of the nanoparticles, acting as coating agents. The preservation of these bands with minimal shifts indicates that certain functional groups were not significantly transformed during the reduction process but remain adsorbed on the surface of the nanoparticles. These residual biomolecules play a key role in improving colloidal stability through steric and electrostatic interactions. [28,29].

Figure 3b shows an enlarged view of the 900–1150 cm^{-1} region, focusing on the absorption band around 1045 cm^{-1} . This band is attributed to C–O–C or C–O stretching vibrations, commonly associated with polysaccharides, glycosides, and other groups present in plant-based stabilizing agents. In the five samples, this band appears consistently, although with greater predominance as the extract volume increases, especially in the sample with 4.0 mL. This trend suggests a higher density of organic compounds adsorbed on the surface of the nanoparticles when a larger amount of extract is used, reinforcing the hypothesis that greater availability of phytochemicals leads to more extensive surface coating. This behavior has also been reported in other green synthesis studies, where higher extract volumes favor nanoparticle dispersion and reduce aggregation [30]. These results confirm that functional groups such as hydroxyls, carbonyls, and ethers present in the extract of *M. nigra* participate in both the reduction of silver ions and the stabilization of AgNPs. The absence of new bands and the persistence of characteristic signals suggest a clean synthesis route, dominated by direct interaction between native plant compounds and metal ions.

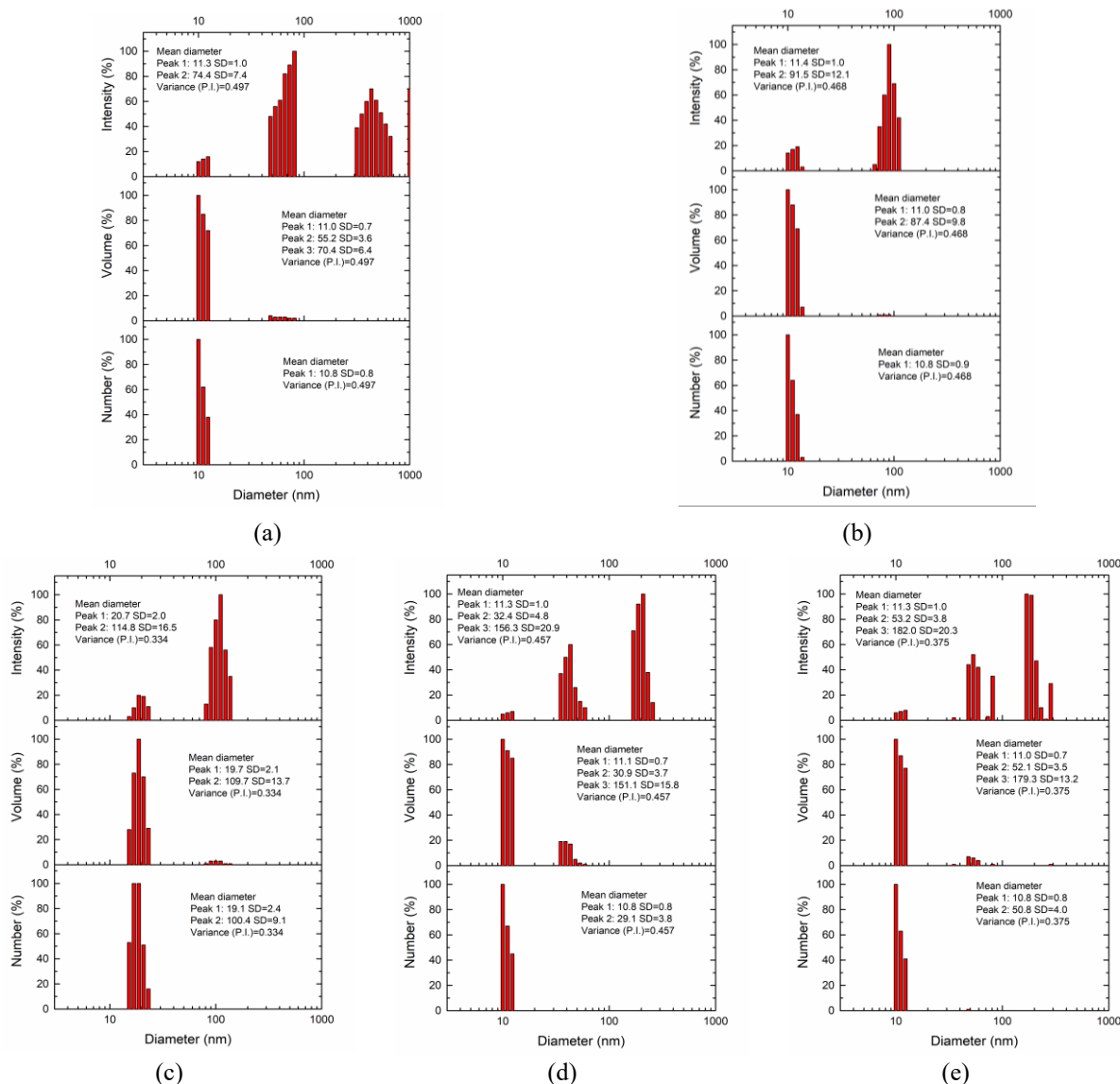


FIGURE 4. DLS for AgNPs synthesized using different volumes of *Morus nigra* extract: (a) 2.0 mL. (b) 2.5 mL. (c) 3.0 mL. (d) 3.5 mL. (e) 4.0 mL.

Characterization by DLS (Figure 4) revealed a notable evolution in the size and distribution of AgNPs as the volume of extract used during synthesis increased. For the 2.0 mL extract volume, although most of the nanoparticles were concentrated around 11 nm, both in number and volume distribution, the analysis revealed a distribution characterized by a polydispersity index (P.I.) of 0.497, suggesting a relatively heterogeneous colloidal population

resulting from a less controlled synthesis, possibly limited by the low concentration of reducing and stabilizing biomolecules present in the extract. When the extract volume was increased to 2.5 mL, a slight improvement in particle uniformity was observed, with a P.I. of 0.468. In the distribution by number and volume, most of the nanoparticles are grouped around 11 nm. These results imply that the 2.5 mL volume begins to establish a more favorable reactive environment, given the greater presence of reducing and stabilizing biomolecules, but is still limited in its ability to completely prevent the formation of agglomerates. For the 3.0 mL volume, a significant improvement in size distribution was observed with a P.I. decreasing to 0.334. The average diameter by number and volume is mostly between 19 and 21 nm. These results suggest that the concentration of biomolecules was sufficient to promote rapid nucleation and prevent excessive growth or aggregate formation. This type of distribution is desirable, especially when nanoparticles with reproducible properties and high specific surface area are sought, which are important for antimicrobial or biomedical applications [31]. The DLS corresponding to the 3.5 mL volume revealed a more complex distribution, with a P.I. of 0.457. Although the number curve showed a dominant peak around 10.8 nm. The increase in P.I. indicate that the system loses homogeneity, despite maintaining the ability to form small nanoparticles. With a volume of 4.0 mL of extract, the system showed a P.I. of 0.375, which in principle would suggest an improvement in uniformity. However, detailed analysis of the distributions reveals greater complexity in the nanoparticle population, with three clearly defined peaks around 11.0 nm, 52.1 nm, and 179.3 nm in volume, and wide standard deviations, especially in the larger fractions. This behavior suggests that, at high volumes, excess reducing and stabilizing biomolecules may generate an oversaturated environment that promotes secondary growth and agglomeration processes, affecting the final distribution. Overall, the results of the DLS analysis show that although lower volumes also favored the formation of small nanoparticles, they exhibited high dispersion and coexistence of multiple sizes. On the other hand, higher volumes showed an increase in system complexity, with the appearance of large fractions associated with an excess of biomolecules, which negatively affected size homogeneity. These findings highlight 3.0 mL as the balance point between reducing efficiency and colloidal stability.

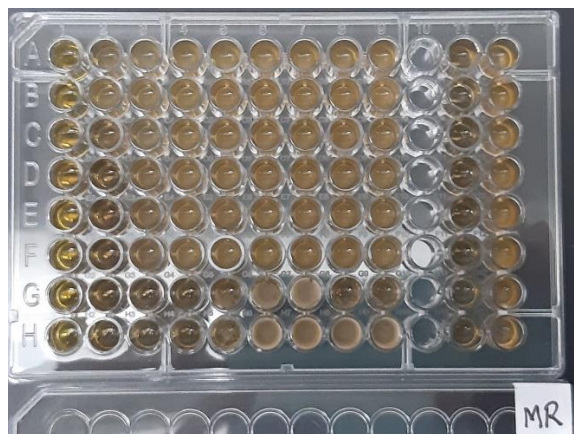


FIGURE 5. 96-well microdilution plate for determining the MIC of silver nanoparticles synthesized with *Morus nigra* extract against *E. coli* (rows A-C), *S. aureus* (rows D-F), and *C. albicans* (rows G and H).

The results obtained in the MIC test (Figure 5) demonstrate that silver nanoparticles (AgNPs) synthesized with 3.0 mL of black mulberry extract have differential antimicrobial activity depending on the type of microorganism evaluated. The lowest MIC was recorded against *Candida albicans* (25%, column 3), followed by *Staphylococcus aureus* (50%, column 2), while for *Escherichia coli*, the full concentration of nanoparticles (100%, column 1) was required to achieve microbial growth inhibition. This sensitivity pattern can be attributed to structural differences in the cell wall of microorganisms. Gram-negative bacteria such as *E. coli* have a lipopolysaccharide outer membrane that acts as a barrier, reducing the penetration of antimicrobial agents, while Gram-positive bacteria such as *S. aureus*, with a more exposed peptidoglycan wall, are generally more susceptible to metal nanoparticles [13,32]. In the case of *C. albicans*, the greater efficacy could be explained by the ability of AgNPs to interact with fungal membranes, altering their permeability and inducing oxidative damage [33]. The black mulberry extract used in the synthesis of the nanoparticles could have contributed phenolic compounds and anthocyanins with intrinsic antimicrobial activity and functioned as reducing agents and stabilizers of the nanoparticles, which is consistent with studies that point to the synergistic effect of polyphenol-rich plant extracts on the antimicrobial activity of AgNPs [2,5]. This synergism may enhance the efficacy of nanoparticles against pathogenic microorganisms. In previous studies, nanoparticles synthesized with extracts from similar fruits, such as blueberry, have also shown low MIC against Gram-positive

bacteria, confirming that the phytochemical characteristics of the extract play a key role in the final activity of the nanoparticles [34]. Furthermore, the size and distribution of nanoparticles, parameters that depend on the concentration of the extract during synthesis, significantly influence the interaction with microorganisms, where smaller particles have a larger surface area and, therefore, a greater antimicrobial effect [35].

CONCLUSION

The green synthesis of silver nanoparticles (AgNPs) with black mulberry fruit extract (*Morus nigra*) yielded spherical and well-dispersed nanoparticles, confirmed by the SPR peak around 420 nm, whose intensity increased with higher extract volumes suggesting greater formation efficiency. However, the shift of the peak to 425 nm and the broadening observed after 6 months reveal a loss of colloidal stability at low volumes, highlighting the need for additional strategies to maintain long-term stability. FTIR analysis showed the participation of hydroxyl and carbonyl groups in the extract in the reduction and stabilization of AgNPs. Size dispersion analysis by DLS indicated that the optimal extract volume for obtaining nanoparticles with better distribution and less agglomeration was 3.0 mL, achieving low polydispersity (PDI = 0.334). In antimicrobial assays, AgNPs obtained with 3.0 mL of extract showed the highest efficacy against *Candida albicans* (MIC=25%) and *Staphylococcus aureus* (MIC=50%), while *Escherichia coli* required the full concentration (100%), confirming a lower susceptibility of Gram-negative bacteria. These results demonstrate that adjusting the volume of black mulberry extract allows for the optimization of the physicochemical properties and antimicrobial activity of AgNPs, supporting their potential as alternative and sustainable antimicrobial agents, although further research into stabilization strategies is recommended to maintain their long-term functionality.

REFERENCES

1. Singh, J., Dutta, T., Kim, K. H., Rawat, M., Samddar, P., & Kumar, P., 'Green' synthesis of metals and their oxide nanoparticles: applications for environmental remediation. *J. Nanobiotechnol.*, 16(1), 84 (2018).
2. Ahmed, S., Ahmad, M., Swami, B. L., & Ikram, S., Green synthesis of silver nanoparticles using *Azadirachta indica* aqueous leaf extract. *J. Radiat. Res. Appl. Sci.*, 9(1), 1-7 (2016).
3. Zhang, X. F., Liu, Z. G., Shen, W., & Gurunathan, S., Silver nanoparticles: synthesis, characterization, properties, applications, and therapeutic approaches. *Int. J. Mol. Sci.*, 17(9), 1534 (2016).
4. Ahmed, S., Ahmad, M., Swami, B. L., & Ikram, S., A review on plants extract mediated synthesis of silver nanoparticles for antimicrobial applications: a green expertise. *J. Adv. Res.*, 7(1), 17-28 (2016).
5. Iravani, S., Green synthesis of metal nanoparticles using plants. *Green Chem.*, 13(10), 2638-2650 (2011).
6. Song, J. Y., & Kim, B. S., Rapid biological synthesis of silver nanoparticles using plant leaf extracts. *Bioprocess Biosyst. Eng.*, 32(1), 79-84 (2009).
7. Mittal, A. K., Chisti, Y., & Banerjee, U. C., Synthesis of metallic nanoparticles using plant extracts. *Biotechnol. Adv.*, 31(2), 346-356 (2013).
8. Chung, I. M., Park, I., Seung-Hyun, K., Thiruvengadam, M., & Rajakumar, G., Plant-mediated synthesis of silver nanoparticles: their characteristic properties and therapeutic applications. *Nanoscale Res. Lett.*, 11(1), 40 (2016).
9. Kumar, B., Smita, K., Cumbal, L., & Debut, A., Green synthesis of silver nanoparticles using Andean blackberry fruit extract. *Saudi J. Biol. Sci.*, 24(1), 45-50 (2017).
10. Nejad, M. S., Najafabadi, N. S., Aghighi, S., Zargar, M., Bayat, M., & Pakina, E., Green synthesis of silver nanoparticles by sweet cherry and its application against cherry spot disease. *Heliyon*, 10(10) (2024).
11. Demirbas, A., Büyükbeziroglu, K., Celik, C., Kislakci, E., Karaagac, Z., Gokturk, E., ... & Ocoy, I., Synthesis of long-term stable gold nanoparticles benefiting from red raspberry (*Rubus idaeus*), strawberry (*Fragaria ananassa*), and blackberry (*Rubus fruticosus*) extracts—gold ion complexation and investigation of reaction conditions. *ACS Omega*, 4(20), 18637-18644 (2019).
12. Dakal, T. C., Kumar, A., Majumdar, R. S., & Yadav, V., Mechanistic basis of antimicrobial actions of silver nanoparticles. *Front. Microbiol.*, 7, 1831 (2016).
13. Rai, M., Yadav, A., & Gade, A., Silver nanoparticles as a new generation of antimicrobials. *Biotechnol. Adv.*, 27(1), 76-83 (2009).
14. Franci, G., Falanga, A., Galdiero, S., Palomba, L., Rai, M., Morelli, G., & Galdiero, M., Silver nanoparticles as potential antibacterial agents. *Molecules*, 20(5), 8856-8874 (2015).
15. Ye, L., Hu, Q., Lin, Y., & Guo, C., Optimizing Fermentation of *Morus nigra* L. Residues with *Schizopyllum commune* to Enhance Anthocyanin Release and Anti-Inflammatory Activity via Pyroptosis Pathway Modulation. *Fermentation*, 11(3), 145 (2025).

16. Khoo, H. E., Azlan, A., Tang, S. T., & Lim, S. M., Anthocyanidins and anthocyanins: Colored pigments as food, pharmaceutical ingredients, and the potential health benefits. *Food Nutr. Res.*, 61(1), 1361779 (2017).
17. Mabry, T., Markham, K. R., & Thomas, M. B., The systematic identification of flavonoids. Springer Science & Business Media (2012).
18. Maqsood, M., Khan, M. I., Sharif, M. K., & Faisal, M. N., Phytochemical characterization of *Morus nigra* fruit ultrasound-assisted ethanolic extract for its cardioprotective potential. *J. Food Biochem.*, 46(11), e14335 (2022).
19. Srikhao, N., Ounkaew, A., Kasemsiri, P., Theerakulpisut, S., Okhawilai, M., & Hiziroglu, S., Green synthesis of silver nanoparticles using the extract of spent coffee used for paper-based hydrogen peroxide sensing device. *Sci. Rep.*, 12(1), 20099 (2022).
20. Al-Asbahi, M. G., Al-Ofiry, B. A., Saad, F. A., Alnehia, A., & Al-Gunaid, M. Q., Silver nanoparticles biosynthesis using mixture of *Lactobacillus* sp. and *Bacillus* sp. growth and their antibacterial activity. *Sci. Rep.*, 14(1), 10224 (2024).
21. Ullah, S., Khalid, R., Rehman, M. F., Irfan, M. I., Abbas, A., Alhoshani, A., ... & Amin, H. M., Biosynthesis of phyto-functionalized silver nanoparticles using olive fruit extract and evaluation of their antibacterial and antioxidant properties. *Front. Chem.*, 11, 1202252 (2023).
22. Haridas, E. S., Varma, M. K., & Chandra, G. K., Bioactive silver nanoparticles derived from *Carica papaya* floral extract and its dual-functioning biomedical application. *Sci. Rep.*, 15(1), 1-14 (2025).
23. Ansari, M., Ahmed, S., Abbasi, A., Khan, M. T., Subhan, M., Bukhari, N. A., ... & Abdelsalam, N. R., Plant mediated fabrication of silver nanoparticles, process optimization, and impact on tomato plant. *Sci. Rep.*, 13(1), 18048 (2023).
24. Amirjani, A., Firouzi, F., & Haghsheenas, D. F., Predicting the size of silver nanoparticles from their optical properties. *Plasmonics*, 15(4), 1077-1082 (2020).
25. Thanh, N. T., Maclean, N., & Mahiddine, S., Mechanisms of nucleation and growth of nanoparticles in solution. *Chem. Rev.*, 114(15), 7610-7630 (2014).
26. Habibullah, G., Viktorova, J., Ulbrich, P., & Ruml, T., Effect of the physicochemical changes in the antimicrobial durability of green synthesized silver nanoparticles during their long-term storage. *RSC Adv.*, 12(47), 30386-30403 (2022).
27. Liu, J., Sonshine, D. A., Shervani, S., & Hurt, R. H., Controlled release of biologically active silver from nanosilver surfaces. *ACS Nano*, 4(11), 6903-6913 (2010).
28. Adeyemi, J. O., Oriola, A. O., Onwudiwe, D. C., & Oyediji, A. O., Plant extracts mediated metal-based nanoparticles: synthesis and biological applications. *Biomolecules*, 12(5), 627 (2022).
29. Agarwal, H., Kumar, S. V., & Rajeshkumar, S., A review on green synthesis of zinc oxide nanoparticles—An eco-friendly approach. *Resour.-Efficient Technol.*, 3(4), 406-413 (2017).
30. Huang, J., Li, Q., Sun, D., Lu, Y., Su, Y., Yang, X., ... & Chen, C., Biosynthesis of silver and gold nanoparticles by novel sundried *Cinnamomum camphora* leaf. *Nanotechnology*, 18(10), 105104 (2007).
31. Rónavári, A., Igaz, N., Adamecz, D. I., Szerencsés, B., Molnar, C., Kónya, Z., ... & Kiricsi, M., Green silver and gold nanoparticles: Biological synthesis approaches and potentials for biomedical applications. *Molecules*, 26(4), 844 (2021).
32. Li, W. R., Xie, X. B., Shi, Q. S., Zeng, H. Y., Ou-Yang, Y. S., & Chen, Y. B., Antibacterial activity and mechanism of silver nanoparticles on *Escherichia coli*. *Appl. Microbiol. Biotechnol.*, 85(4), 1115-1122 (2010).
33. Kim, K. J., Sung, W. S., Suh, B. K., Moon, S. K., Choi, J. S., Kim, J. G., & Lee, D. G., Antifungal activity and mode of action of silver nano-particles on *Candida albicans*. *Biomaterials*, 22(2), 235-242 (2009).
34. Plesnicute, R., Rimbu, C., Oprica, L., Herea, D., Motrescu, I., Luca, D., ... & Grigore, M. N., Eco-Friendly Synthesis of Silver Nanoparticles with Significant Antimicrobial Activity for Sustainable Applications. *Sustainability*, 17(12), 5321 (2025).
35. Loo, Y. Y., Rukayadi, Y., Nor-Khaizura, M. A. R., Kuan, C. H., Chieng, B. W., Nishibuchi, M., & Radu, S., In vitro antimicrobial activity of green synthesized silver nanoparticles against selected gram-negative foodborne pathogens. *Front. Microbiol.*, 9, 1555 (2018).